High Resolution Transmission Electron Microscope Observation of Zero-Strain Deformation Twinning Mechanisms in Ag

L. Liu,[1] J. Wang,[2,*] S. K. Gong,[1,†] and S. X. Mao[3,‡]

[1]School of Materials Science and Engineering, Beihang University, Beijing 100191, People's Republic of China
[2]MST-8, MS G755, Los Alamos National Laboratory, Los Alamos, New Mexico 87545, USA
[3]Department of Mechanical Engineering and Materials Science, University of Pittsburgh, Pittsburgh, Pennsylvania 15261, USA

(Received 2 February 2011; published 29 April 2011)

We have observed a new deformation-twinning mechanism using the high resolution transmission electron microscope in polycrystalline Ag films, zero-strain twinning via nucleation, and the migration of a $\Sigma 3\{112\}$ incoherent twin boundary (ITB). This twinning mechanism produces a near zero macroscopic strain because the net Burgers vectors either equal zero or are equivalent to a Shockley partial dislocation. This observation provides new insight into the understanding of deformation twinning and confirms a previous hypothesis: detwinning could be accomplished via the nucleation and migration of $\Sigma 3\{112\}$ ITBs. The zero-strain twinning mechanism may be unique to low staking fault energy metals with implications for their deformation behavior.

DOI: 10.1103/PhysRevLett.106.175504 PACS numbers: 62.20.F−

Twinning is a typical plastic deformation mechanism, accomplished by the glide of twinning dislocations (TDs) to generate macroscopic strain [1,2]. Deformation twinning has been widely observed in materials with different crystal structures, such as body-centered-cubic (bcc) [1], face-centered-cubic (fcc) [3–8], hexagonal-close-packed (hcp) [9–13], and others [14–16]. For fcc metals, the tendency of deformation twinning is mainly determined by its stacking fault energy (SFE) [17]. For fcc metals with medium-to-high SFEs such as Cu and Al, dislocation slip is the preferred plastic deformation mechanism for coarse-grained metals. For fcc metals with low SFE like Ag, plastic deformation is accomplished by a combination of dislocation slip and deformation twinning [18]. Many twinning mechanisms have been proposed, including the pole mechanisms [19], prismatic glide [20], faulted dipole [16], and others [14,15]. These deformation twins are accomplished by the glide of TDs. TDs usually all have the same Burgers vector so that the Peach-Koehler glide forces on the TDs have the same sign and they move along the same direction [2]. As a consequence of twin propagation, a net macroscopic strain is generated.

Is it true that deformation twinning always produces a net macroscopic strain? Recently, Wu *et al.* proposed a new twinning mechanism, random activation of partials (RAP), to explain the zero net macroscopic strain phenomena associated with twinning in nanocrystalline Al, Ni, and Cu [21]. It is noticed that since the participating Burgers vectors sum to zero in the random activation of partials mechanism, RAP twinning must produce zero net macroscopic strain. More recently, Wang *et al.* reported their *in situ* TEM observation and revealed a new detwinning mechanism in Cu, in which detwinning is accomplished via the collective glide of $\Sigma 3\{112\}$ incoherent twin boundaries (ITBs) [22–25]. Since $\Sigma 3\{112\}$ ITBs can be presented with a set of Shockley partial dislocations with a repeatable sequence $b_2{:}b_1{:}b_3$ on every (111) plane [22], a noteworthy characteristic of the three partial dislocations is that the sum of their Burgers vectors in one unit equals zero [22,23]. Accompanying with detwinning in Cu, the net macroscopic strain must be zero. Some analogous mechanisms had been postulated by Christian who explained the fcc to hcp transformation in metals [26] and by Mahajan *et al.* [27] to explain the formation for annealing twins.

It is still a puzzle why such twin boundaries (front tip of deformation twins) move under zero or very small net Peach-Koehler force due to the zero net Burgers vectors. It was understood that the transformation [26] and annealing twinning [27] can be driven by the Gibbs free energy difference, and the detwinning mechanisms for thin twin lamellae can be driven by reducing the area of twin boundaries [25]. Comparing with the above mechanisms [25–27], deformation twinning through the mechanisms in Refs. [21,25] will create new high-energy twin boundaries; thus, it is not energetically favorable. To explain the motion of such boundaries, Wang *et al.* propose a stop-start, move-drag, partial dislocation mechanism [25], in which $\Sigma 3\{112\}$ ITB goes from an equilibrium state to a nonequilibrium state, then back to an equilibrium state again. They also observed that ITBs could be pinned due to the interaction of lattice dislocation with ITBs using *in situ* TEM [24]. But the experimental evidence is still insufficient corresponding to deformation twinning via the collective glide of ITBs.

In this Letter, we report deformation-twinning mechanisms, with a focus on zero-strain deformation twinning, in polycrystalline Ag films. High purity 99.99% silver films with a thickness of 1 mm were used for the experiment. Annealing was carried out at 1073 K, less than 10^{-4} Pa to eliminate crystalline defects. After annealing, the films

were cooled in liquid nitrogen, and then immediately rolled to 50 μm thickness (95% rolling strain) at room temperature. The 3 mm diameter transmission electron microscope (TEM) specimen was cut from the films and thinned by double-jet electropolishing in solution of 10% perchloric acid, 10% glycerol, and 80% methanol at 213 K in a TenuPol-5 electropolisher. TEM observation was conducted using a JEM2100F microscope with a point-to-point resolution of 0.23 nm.

Figure 1(a) is taken after annealing, showing no twins while dislocation lines can be observed, although minor annealing twins have been found elsewhere. After mechanical rolling, Figs. 1(b) and 1(c) show a lot of twins observed in grains (the grain size $\sim$1 μm). These twins have an average thickness of 50–60 nm and two types of twin boundaries, $\Sigma 3\{111\}$ coherent twin boundaries (CTBs) and $\Sigma 3\{112\}$ incoherent twin boundaries (ITBs).

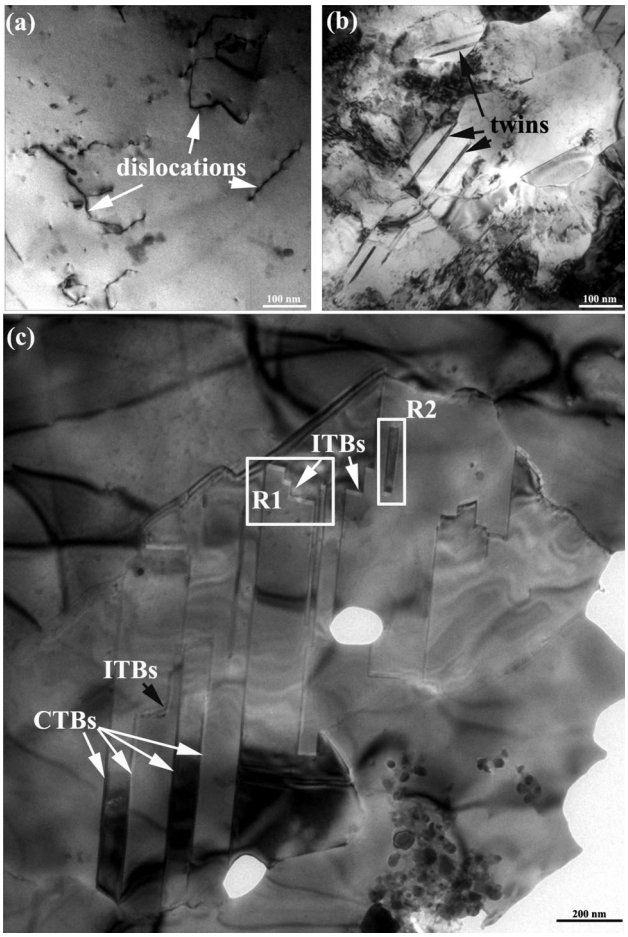

FIG. 1. (a) TEM image of the silver after annealing. (b) and (c) TEM images of the silvers at grain size ($\sim$ 1 μm) after cold rolling to 95% strain, showing twins with the average twin thickness of 50–60 nm, and two types of twin boundaries: coherent twin boundaries (CTBs) and incoherent twin boundaries (ITBs). For most twins, one of two ends is at grain boundary and the other end is inside of grains. Two regions, $R1$ and $R2$ in (c) are marked for further analysis.

For most twins, one of two ends is at grain boundary and the other end is inside of grains. Dislocation debris has been found in another area under HRTEM although Fig. 1(c) shows dislocation free with the regular TEM image. Two regions in Fig. 1(c) are marked for further analysis. It is worth mentioning that the region $R2$ shows a twin with both ends inside of the grain.

To identify the characteristics of the front tips of deformation twins, HRTEM analysis is conducted for regions $R1$ and $R2$ [Fig. 1(c)]. It is noted that (1) a repeated pattern with the periodicity of 3 times the interplanar spacing of $\{111\}$ planes is clearly observed [Figs. 2(b), 2(c), and 2(e)], (2) the $9R$ structure is bounded between the two phase boundaries [23], PB1 and PB2 [Figs. 2(b) and 2(e)], and (3) the extra spots compared to regular fcc $\langle 110\rangle$ SAED [Fig. 2(f)]. All of these points confirm that the ends of twins are $\Sigma 3\{112\}$ ITBs. In addition, the most intriguing result from the TEM analysis of $R2$ is that the twin has $\Sigma 3\{112\}$ ITBs as both ends, which supports our hypothesis that deformation twins can propagate with the front end as $\Sigma 3\{112\}$ ITBs; i.e., the sum of Burgers vectors of partials at the front equals zero.

However, it is not clear whether these twins are experiencing twinning processes or detwinning processes. Figure 3 shows a series of TEM images containing a twin end—$\Sigma 3\{112\}$ ITB. The width of the $9R$ structure is initially measured about 12.5 nm, then reduces to 4.5 nm and finally is stabilized at 1.2 nm, which is close to the equilibrium distance of 1.0 nm at zero applied shear stress [23]. It is worth mentioning that (1) PB1 moves downward, (2) PB2 moves upward, but (3) PB2 moves slower than PB1. This collapse process can be ascribed to the relaxation of the preexisting internal stresses within observation time. Accompanying the relaxation of internal stresses, the initial equilibrium on the force applied to partials can be destroyed, resulting in the glide of both boundaries. The moving distances for PB1 about 10 nm downward and for PB2 1.0 nm upward, implying that PB2 experiences a higher Peierls force than PB1. To address the influence of the local shear stress on $\Sigma 3\{112\}$ ITBs, we conducted molecular dynamics simulations for Ag. As shown in Fig. 3(d), owing to the mirror symmetry of two crystals across a twin boundary, Shockley partial dislocations b_1 could be in the left or the right side of the boundary PB2 at zero applied shear stress. At a certain applied shear stress, Shockley partial dislocations b_1 can be in only one side corresponding to the Peach-Koehler force, for example, the lower configuration in Fig. 3(d). In other words, the position of PB1 serves as a flag, indicating the propagation of a twin along the twinning direction or along the opposite direction corresponding to detwinning. Combining *in situ* TEM results with atomistic simulations, we can find that (1) internal stresses exist in the rolled Ag films in Figs. 2 or 3(a), and (2) the net Peach-Koehler force acting on the Shockley partials b_1 (PB1) towards the twinning direction,

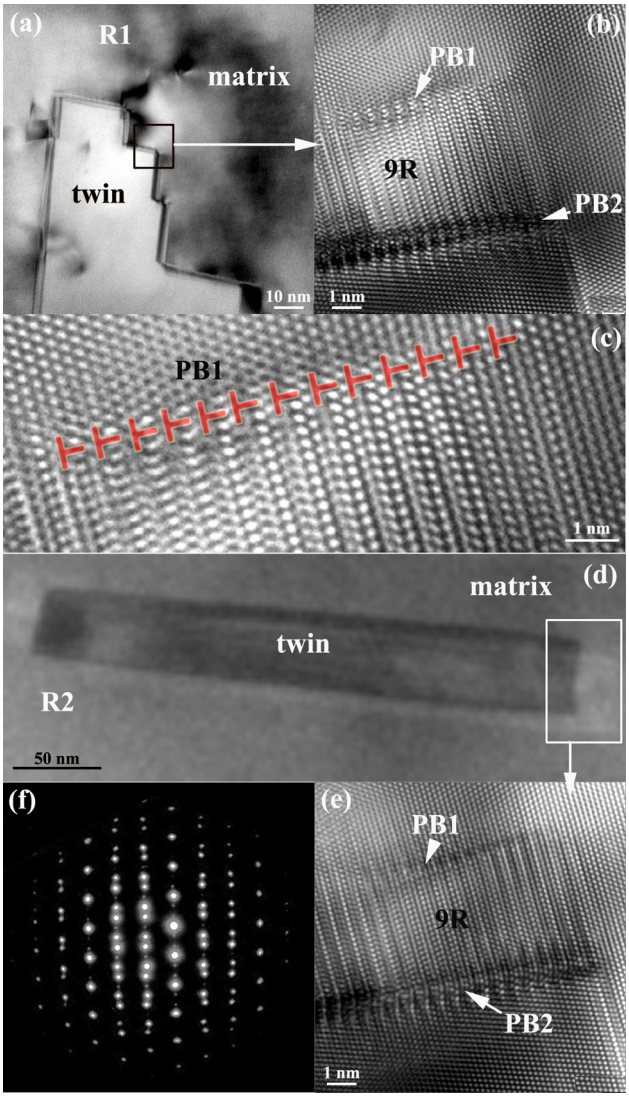

FIG. 2 (color online). Characterization of the front end of deformation twins. (a), (b), and (c) correspond to $R1$ in Fig. 1(c): (a) the magnification, (b) HRTEM image of the front end composed of PB1, 9R, and PB2, and (c) the magnification of PB1 shows Shockley partial dislocations separated by every three atom planes. (d) and (e) correspond to $R2$ in Fig. 1(c): (d) the magnification, and (e) HRTEM image of one end of the deformation twin, showing a wider ITB composed of PB1, 9R, and PB2. In (b) and (e), PB1 represents an array of Shockley partial dislocations b_1 separated by every two {111} atomic planes act as the front tip of the deformation twins; PB2 represents an array of Shockley partial dislocations separated by every one {111} atomic plane with a consequence b_2:b_3 in the boundary of the twin and 9R structure. (f) ⟨110⟩ SAED pattern corresponding to (e) shows the extra spots in comparison with a normal fcc structure. The symbol "⊥" indicates Shockley partial dislocations b_1 in the PB1.

implying that the deformation twins observed in Ag are experiencing a twinning process.

Coupling atomistic simulations and experimental observations, we here discuss the motion mechanism of

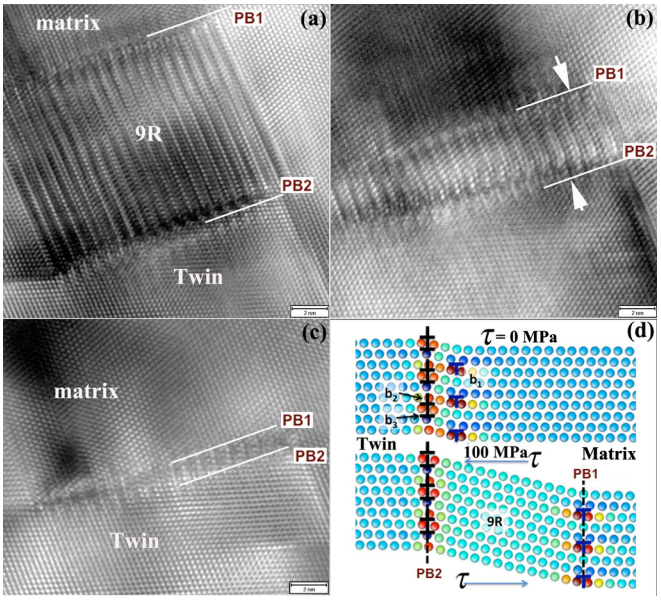

FIG. 3 (color online). A series of snapshots showing the collapse of 9R structure during TEM observation, from (a) initial 12.5 nm, to (b) 4.0 nm, to (c) a stable size of 1.2 nm. The collapse of 9R structure is accomplished via the glide of PB1 and PB2. PB1 moves 10 nm downward and PB2 1.0 nm upward from (a) to (c). (d) Atomic structures of $\Sigma 3\{112\}$ ITBs in Ag. The top shows the equilibrium structure at zero applied shear stress and the lower at the applied shear stress of 100 MPa.

ITBs. When the ITB is subjected to a shear stress τ, the Peach-Koehler glide force on the partial dislocation b_1 is composed of the contribution of the applied shear stress, the contributions of dislocation interactions, the interface tension arising from the stacking fault, and any Peierls force or other friction type force. The Peierls force may be negligible for b_1, typical of isolated partials in fcc metals [2]. However, a Peierls force may be present for the paired partials b_2 and b_3 [illustrated in Fig. 3(d)], as implied by *in situ* TEM observation (Fig. 3), because they remain closely spaced in the residual ITB and may correspond to a relaxed nonlinear structure (the paired partials are hard to break away from each other due to the attractive force originating from the interaction of their screw components). When the ITB (containing three types of dislocations), whether compact or dissociated, is in the equilibrium state, the net force equals zero regardless of the magnitude of the applied shear stresses. For the near equilibrium state, a slight increase in stress would move the partial dislocation b_1, because the partial dislocation b_1 is initially more mobile than the other two partial dislocations [22]. For the first scenario an increased stress is required for the partial dislocation b_1 to overcome the interaction force, but the latter drops as it moves tending to produce breakaway at constant stress. However, locally the plastic strain associated with the motion of the partials should produce a load drop, tending to arrest the motion of partial b_1. The load drop would be permanent under constant

applied strain, or temporary (over a period where an elastic wave reaches the remote free surface and returns) under constant applied load. Then the paired partials (b_2 and b_3) would have SFE plus the interaction force pulling them and decreased applied force acting on the paired partials so they could move to approach the b_1 partial until again reaching the equilibrium spacing. This process could repeat, resulting in the migration of ITBs in the direction favored by the applied force acting on the b_1 partials, during which zero deformation twin is developed. Locally, the situation would represent a stop-start, jump-drag displacement situation with some waiting time [25].

It is worthwhile to discuss the nucleation of such zero-strain deformation twins. As observed in TEM images, most deformation twins originate at grain boundaries. Similar to a grain boundary nucleation mechanism in nanocrystalline materials [21] and a dissociation mechanism of grain boundary dislocations in Mg [28,29], the nucleation of a deformation twin with $\Sigma 3\{112\}$ ITBs as its front tip may require some structural characteristics of the grain boundary, for example, the grain boundary is close to $\Sigma 3\{112\}$ ITBs, then dissociate to one $\Sigma 3\{112\}$ ITB and the other grain boundary. Further TEM studies are required to address the structural characteristics of grain boundaries.

In a summary, we have observed a new deformation-twinning mechanism using HRTEM in polycrystalline Ag films, twinning via the migration of $\Sigma 3\{112\}$ ITBs. As a result of the net zero Burgers vector at the twin front, this twinning mechanism does not produce macroscopic strain. This observation provides evidence for our previous hypothesis (detwining could be accomplished via the nucleation and migration of $\Sigma 3\{112\}$ incoherent twin boundary at grain boundaries) [25], and opens new insight into the understanding of deformation twinning, especially the effect of atomic structures of grain boundaries [28,29] and at or near crack tip [30].

S. G. acknowledges the support from NSFC No. 50731001. J. W. acknowledges the support provided by the Center for Materials at Irradiation and Mechanical Extremes, an Energy Frontier Research Center funded by the U.S. Department of Energy, Office of Science, Office of Basic Energy Sciences under No. 2008LANL1026, and also acknowledge support provided by the Los Alamos National Laboratory Directed Research and Development (LDRD). S. M. would like to acknowledge NSF CMMI 08 010934 through the University of Pittsburgh.

*wangj6@lanl.gov
†gongsk@buaa.edu.cn
‡smao@engr.pitt.edu

[1] J. W. Christian and S. Mahajan, Prog. Mater. Sci. **39**, 1 (1995).
[2] J. P. Hirth and J. Lothe, *Theory of Dislocations* (Krieger, Melbourne, FL, 1992).
[3] V. Yamakov, D. Wolf, S. R. Phillpot, and H. Gleiter, Acta Mater. **50**, 5005 (2002).
[4] Z. W. Shan, L. Lu, A. M. Minor, E. A. Stach, and S. X. Mao, JOM **60**, 71 (2008).
[5] E. Ma, Y. M. Wang, Q. H. Lu, M. L. Sui, L. Lu, and K. Lu, Appl. Phys. Lett. **85**, 4932 (2004).
[6] J. Wang and H. Huang, Appl. Phys. Lett. **88**, 203112 (2006).
[7] M. W. Chen, E. Ma, K. J. Hemker, H. W. Sheng, Y. M. Wang, and X. M. Cheng, Science **300**, 1275 (2003).
[8] X. Z. Liao, Y. H. Zhao, S. G. Srinivasan, Y. T. Zhu, R. Z. Valiev, and D. Gunderov, Appl. Phys. Lett. **84**, 592 (2004).
[9] L. Wang, P. Eisenlohr, Y. Yang, T. R. Bieler, and M. A. Crimp, Scr. Mater. **63**, 827 (2010).
[10] L. Wang, Y. Yang, P. Eisenlohr, T. R. Bieler, M. A. Crimp, and D. E. Mason, Metall. Mater. Trans. A **41**, 421 (2009).
[11] C. N. Tomé and G. C. Kaschner, Mater. Sci. Forum **495–497**, 1001 (2005).
[12] J. Wang, J. P. Hirth, and C. N. Tomé, Acta Mater. **57**, 5521 (2009).
[13] J. Wang, R. G. Hoagland, J. P. Hirth, L. Capolungo, I. J. Beyerlein, and C. N. Tomé, Scr. Mater. **61**, 903 (2009).
[14] S. Mahajan and G. Y. Chin, Acta Metall. **21**, 1353 (1973).
[15] N. Thompson, Proc. Phys. Soc. London Sect. B **66**, 481 (1953).
[16] M. Niewczas and G. Saada, Philos. Mag. A **82**, 167 (2002).
[17] H. Van Swygenhoven, P. M. Derlet, and A. G. Frøseth, Nature Mater. **3**, 399 (2004).
[18] E. B. Tadmor and N. Bernstein, J. Mech. Phys. Solids **52**, 2507 (2004).
[19] A. Ookawa, J. Phys. Soc. Jpn. **12**, 825 (1957).
[20] J. A. Venables, Philos. Mag. A **6**, 379 (1961).
[21] X. L. Wu, X. Z. Liao, S. G. Srinivasan, F. Zhou, E. J. Lavernia, R. Z. Valiev, and Y. T. Zhu, Phys. Rev. Lett. **100**, 095701 (2008).
[22] J. Wang, O. Anderoglu, J. P. Hirth, A. Misra, and X. Zhang, Appl. Phys. Lett. **95**, 021908 (2009).
[23] J. Wang, A. Misra, and J. P. Hirth, Phys. Rev. B **83**, 064106 (2011).
[24] N. Li, J. Wang, J. Y. Huang, A. Misra, and X. Zhang, Scr. Mater. **64**, 149 (2011).
[25] J. Wang, N. Li, O. Anderoglu, X. Zhang, A. Misra, J. Y. Huang, and J. P. Hirth, Acta Mater. **58**, 2262 (2010).
[26] J. W. Christian, *The Theory of Transformations in Metals and Alloys* (Pergamon, New York, 1965).
[27] S. Mahajan, C. S. Pande, M. A. Imam, and B. B. Rath, Acta Mater. **45**, 2633 (1997).
[28] J. Wang, I. J. Beyerlein, and C. N. Tomé, Scr. Mater. **63**, 741 (2010).
[29] I. J. Beyerlein and C. N. Tomé, Proc. R. Soc. A **466**, 2517 (2010).
[30] B. Q. Li, B. Li, Y. B. Wang, M. L. Sui, and E. Ma, Scr. Mater. **64**, 852 (2011).